



## Form Factors of Chiral Primary Operators at Two Loops in ABJ(M)

Young, D

For additional information about this publication click this link.

<http://qmro.qmul.ac.uk/jspui/handle/123456789/8208>

Information about this research object was correct at the time of download; we occasionally make corrections to records, please therefore check the published record when citing. For more information contact [scholarlycommunications@qmul.ac.uk](mailto:scholarlycommunications@qmul.ac.uk)

# Form Factors of Chiral Primary Operators at Two Loops in ABJ(M)

Donovan Young

*NORDITA*

*KTH Royal Institute of Technology and Stockholm University  
Roslagstullsbacken 23, SE-10691 Stockholm, Sweden*

donovany@nordita.org

## Abstract

We calculate the colour-ordered form factor for chiral primary operators built from  $J$  scalar fields of ABJ(M) theory to  $J$  scalar final states. We work in the 't Hooft limit and show that the leading quantum correction is  $\mathcal{O}(\lambda^2)$ , where  $\lambda$  is the 't Hooft coupling. We evaluate this leading correction using standard Feynman diagrams and dimensional regularization, and find that the leading divergence is  $1/\epsilon^2$  where the spacetime dimension is  $d = 3 - 2\epsilon$ . We further find that the result respects maximal transcendentality.

# Contents

<b>1</b>	<b>Introduction</b>	<b>1</b>
<b>2</b>	<b>ABJ(M) form factors</b>	<b>3</b>
2.1	One loop is zero . . . . .	4
2.2	Two-loop analysis: $J = 2$ case . . . . .	5
2.2.1	Colour factors . . . . .	8
2.2.2	Assembling the result . . . . .	9
2.3	$J > 2$ case . . . . .	10
2.3.1	Flavour structure for $I_{10}$ . . . . .	12
2.3.2	Assembling the result . . . . .	12
<b>3</b>	<b>Discussion</b>	<b>13</b>
<b>A</b>	<b>Computational details</b>	<b>14</b>
A.1	Effective rule for $I_4$ . . . . .	16
A.2	Effective rule for $I_8$ . . . . .	16
A.3	On the vanishing of certain diagrams . . . . .	17

## 1 Introduction

The study of scattering amplitudes has emerged as a new direction of research in the AdS/CFT correspondence. The discoveries of the twistor string description, BDS ansatz, null-polygonal Wilson loop equivalence, recursion relations, unitarity-based techniques, colour-kinematics duality, Yangian symmetry, Grassmannian formulation, and the relation between gauge theory and gravity amplitudes have together founded a new research area, sometimes referred to as amplitudeology (see [1] chapter V for a review and partial list of references).

Traditionally, the main objects of interest on the CFT side of the AdS/CFT correspondence have been gauge invariant local operators. Non-local operators have also been studied. For example Wilson loops have received wide attention, and surface operators have also been investigated. But until relatively recently, scattering amplitudes had been studied less. Indeed, it is unnatural to consider scattering amplitudes in a CFT, since the absence of asymptotic states precludes their definition. This can be overcome through dimensional regularization: the introduction of an IR regularization  $d = d_0 - 2\epsilon$  with  $\epsilon < 0$  allows amplitudes to be calculated and their divergences as  $\epsilon \rightarrow 0$ , at least in the case of  $\mathcal{N} = 4$  supersymmetric Yang-Mills theory (SYM) in four dimensions, display a beautiful structure captured by exponentiation and the appearance of the cusp anomalous dimension [2]. On the string side of the correspondence Alday and Maldacena [3] showed that this IR regularization corresponds to the introduction of a brane deep in the bulk of AdS on which the scattering is taking place. A T-duality operation which inverts the bulk direction (and hence swaps IR and UV divergences) maps the process to a fundamental string with minimal embedding having a null-polygon on the AdS boundary as its own boundary,

i.e. the string-dual to a null-polygonal Wilson loop in the gauge theory. The full extent of this T-duality symmetry is reflected in dual-superconformal symmetry [4], where the  $PSU(2, 2|4)$  symmetry group of  $\mathcal{N} = 4$  SYM is doubled, and a Yangian symmetry emerges from this structure [5]. Since Yangians are fundamental structures in integrable systems, it would appear that the famed integrability of  $\mathcal{N} = 4$  SYM as applied to the two-point functions of local operators (i.e. the spectral problem) may be emerging also in the study of scattering amplitudes.

It is highly desirable to make links with the program of integrability outside the application to the spectral problem. In this spirit the question of how integrability impacts higher-point correlation functions of local operators, such as three-point functions, has begun to receive attention. In the case of the  $AdS_4/CFT_3$  correspondence between  $\mathcal{N} = 6$  superconformal Chern-Simons theory (ABJM) and M-theory on  $AdS_4 \times S^7/\mathbb{Z}_k$  [6], the question of three-point functions offers a unique opportunity. Both the usual spectral-problem integrability and the Yangian invariance of scattering amplitudes appears to be present in ABJM, and thus we can also ask what impact integrability may have on the three-point functions. The most basic local operators are the chiral primaries (CPO's) – these are symmetrized traces of scalar fields, and have protected conformal dimensions. In the case of  $\mathcal{N} = 4$  the three-point functions of the chiral primaries are also protected, indeed they are independent of the coupling. The same, however, is not true in ABJM. The three-point functions of chiral primaries have non-trivial coupling dependence and an interesting structure of contractions between the symmetric-traceless tensors which define them<sup>1</sup>; at strong coupling supergravity indicates that they scale as  $\lambda^{1/4}/N$ , where  $\lambda = N/k$  is the ABJM 't Hooft coupling [8]. The interpolating function governing the three-point function of CPO's in ABJM stands a good chance of being a simple, fundamental quantity in the  $AdS_4/CFT_3$  correspondence, and it would not be surprising to find that it is related to something which integrability could compute. Of course, it might also be related to the scaling function  $h(\lambda)$ , which is undetermined by integrability, but might be provided via localization techniques [9, 10].

Form factors offer a bridge between traditional local gauge-invariant operator correlation functions and scattering amplitudes, and could help elucidate the connection between the integrable and other structures found in each case. Perhaps more importantly, they are easier to compute than correlation functions, and, as recently demonstrated [11], may be used to construct higher-point correlation functions using generalized unitarity. The form factor calculations presented here serve as a basis both to study these objects further in their own right and as a tool to build correlation functions, especially the three-point functions of CPO's, in perturbation theory, which the author hopes to report upon in the near future.

Form factors have been studied in the context of  $\mathcal{N} = 4$  SYM in a series of papers. The founding paper [12] studied length-2 CPO form factors with two scalar final states to two loops, where exponentiation of IR divergences, controlled by the cusp and collinear anomalous dimensions as in the case of amplitudes, and further exponen-

---

<sup>1</sup>We also note that extremal n-point functions of CPO's have been computed in the free field theory limit of ABJ(M) in [7].

tiation of the finite part was noted. Links to Parke-Taylor structure at tree-level were developed in [13]. More recently the length-2 CPO form factor [14–16] and length- $n$  CPO form factor [17, 18] have been studied with a general number of gluons in the final states in MHV and more general configurations, where exponentiation of divergences continues to be present, while a remainder function for the finite part appears for the first time for three external states. This remainder function has been evaluated at the two-loop level and displays some intriguing connections to the maximally transcendental part of an analogous QCD calculation [16]. Supersymmetrization of both the length-2 operator, in the sense of replacing it with the entire stress-energy multiplet of operators, and the final states has also been accomplished [15, 18], while recursion relations and (dual) MHV rules for the form factors have been developed in [15]. The form factor for the Konishi state has also been considered in [17].

In this paper we calculate the leading quantum correction in the 't Hooft limit to the form factors for chiral primary operators of length  $J$ , with  $J$  scalar final states, in the  $\mathcal{N} = 6$  superconformal Chern-Simons theory known as ABJ(M) [6, 19]. We show that the leading correction is at the two-loop level, and reduce the relevant Feynman diagrams to master integrals. Our results are contained in (2.14), (2.16) and (2.22), (2.25) for the  $J = 2$  and  $J > 2$  cases respectively. The  $J = 2$  case in the ABJM theory has been concurrently computed via generalized unitarity in [20]. Our (2.14) matches this result to all orders in  $\epsilon$ . The form factors diverge as  $\mathcal{O}(\epsilon^{-2})$ , and respect the principle of maximal transcendentality.

The paper is organized as follows. In section 2 we introduce and define the form factors, show that the one-loop correction vanishes, and calculate the two-loop result first for the  $J = 2$  case, which has some special subtleties owing to the colour structure of the diagrams, and then for the  $J > 2$  cases. We conclude with a short discussion in section 3. Conventions, Feynman rules, and some other details of the calculation may be found in the appendix.

## 2 ABJ(M) form factors

We would like to compute the leading perturbative correction to the form factor of a chiral primary operator built of scalar fields  $Y^A$  and  $Y_A^\dagger$ , given by

$$\mathcal{O}_A^J = (\mathcal{C}_A)_{B_1 \dots B_{J/2}}^{A_1 \dots A_{J/2}} \text{Tr} \left( Y^{B_1} Y_{A_1}^\dagger \dots Y^{B_{J/2}} Y_{A_{J/2}}^\dagger \right), \quad (2.1)$$

where  $\mathcal{C}_A$  is completely symmetric in upper and (independently) in lower indices, while the trace taken on any pair consisting of one upper and one lower index vanishes. The tensors are orthonormal, so that

$$(\mathcal{C}_A)_{K_1 \dots K_{J/2}}^{I_1 \dots I_{J/2}} (\mathcal{C}_B^*)_{I_1 \dots I_{J/2}}^{K_1 \dots K_{J/2}} = \delta_{AB}, \quad (2.2)$$

and the two-point function, i.e. the conformal dimension of the operator, is protected against quantum corrections by supersymmetry.

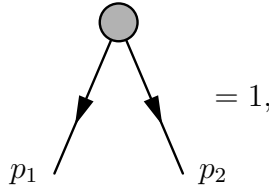
The colour-ordered form factor  $F(\{s_{ij}\})$  we consider is for the production of scalar final states, and is defined by the following expression<sup>2</sup>

$$\begin{aligned} \frac{J}{2} (\mathcal{C}_A)_{B_1 \dots B_{J/2}}^{A_1 \dots A_{J/2}} F(\{s_{ij}\}) \\ \equiv \left\langle Y^{A_1}(p_1) Y_{B_1}^\dagger(p_2) \cdots Y^{A_{J/2}}(p_{J-1}) Y_{B_{J/2}}^\dagger(p_J) \left| \mathcal{O}_A^J(0) \right| 0 \right\rangle, \end{aligned} \quad (2.3)$$

where  $s_{ij} = (p_i + p_j)^2$  are the Mandelstam invariants associated with the on-shell (i.e.  $p_i^2 = 0$ ) external legs. This definition has been chosen so that the tree-level result is  $F(\{s_{ij}\}) = 1$ . To begin with we specialize to the  $J = 2$  case, as many of the diagrams will simply be recycled across the extra legs in the  $J > 2$  cases.

## 2.1 One loop is zero

We represent the tree-level result in the following diagrammatic language (e.g. for  $J = 2$ )



so that the gray blob at the top represents the operator, and final state momenta are outgoing. The one-loop correction to the form factor vanishes. It is given by the one-gluon exchange between adjacent legs, depicted below for the  $J = 2$  case

$$\propto \int \frac{d^3 q}{(2\pi)^3} \frac{\epsilon_{\mu\nu\rho} q^\mu p_1^\nu p_2^\rho}{q^2 (q + p_1)^2 (q - p_2)^2} = 0.$$

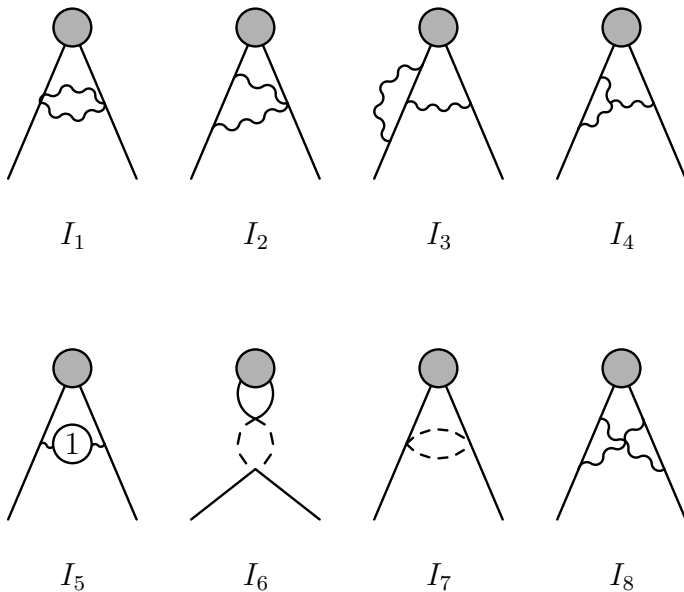
This vanishes under the integration of the loop momentum because of the integrand being an odd function of the loop momentum. A more general argument for the vanishing of these types of diagrams on the physical dimension is given in appendix A.3.

---

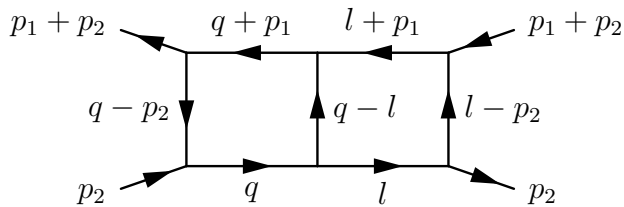
<sup>2</sup>We suppress the gauge group indices. To restore them note that  $Y^{A_a} \rightarrow (Y^{A_a})_{i_a \hat{i}_a}$ ,  $Y_{B_a}^\dagger \rightarrow (Y_{B_a}^\dagger)_{\hat{j}_a j_a}$  and so the LHS of (2.3) should carry a factor of  $\prod_{a=1}^{J/2} \delta_{i_{a+1} \hat{j}_a} \delta_{i_a \hat{j}_a}$ , where  $a \sim a + J/2$ .

## 2.2 Two-loop analysis: $J = 2$ case

We find that the following diagrams contribute at two-loop order (wiggly line = gluon, dashed line = fermion, plain line = scalar)

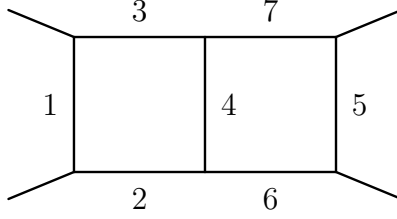


These diagrams also appear in [21], where effective Feynman rules for them have been given. These rules are reproduced here in appendix A, along with supplementary details of the calculation, action, conventions etc. for convenience. The effective Feynman rules come from replacing momentum contractions involving the three-dimensional Levi-Civita tensor with usual scalar (i.e. dot) products. We then use these scalar products to remove propagators from a scalar “master topology” diagram; the results are then reduced to master integrals using the Laporta algorithm [22]. It may seem surprising to see in  $I_8$  a non-planar-looking diagram<sup>3</sup>, even though we are working in the large- $N$  limit: since one of the gluons may travel around the outside of the operator, the diagram is in fact planar. The colour structure will be discussed in greater detail below. Diagram  $I_6$  is trivial to evaluate and we will consider it later. Apart from  $I_8$  which requires a different treatment, the remaining diagrams may all be expressed in terms of the following master topology



where we label propagators as follows

<sup>3</sup>We have verified that the “un-crossed” version of  $I_8$  is exactly zero; an argument for it being  $\mathcal{O}(\epsilon)$  or smaller is given in appendix A.3.



This allows us to express all terms in the Feynman rules in terms of the integral

$$G(n_1, n_2, n_3, n_4, n_5, n_6, n_7) = \int \frac{d^{2\omega} q}{(2\pi)^{2\omega}} \int \frac{d^{2\omega} l}{(2\pi)^{2\omega}} [(q - p_2)^2]^{-n_1} [q^2]^{-n_2} [(q + p_1)^2]^{-n_3} [(q - l)^2]^{-n_4} [(l - p_2)^2]^{-n_5} [l^2]^{-n_6} [(l + p_1)^2]^{-n_7}. \quad (2.4)$$

Take for example  $I_1$ , this diagram has  $n_1 = n_3 = n_6 = 0$  prior to consideration of the numerator. Using the first rule in appendix A [21] we see that the numerator is a scalar product of the two momenta (those labeled by 2 and 4 in the master topology) carried by the two gluons in the diagram. We reexpress this scalar product in terms of  $(p_1 + p_2)^2$  and the squared momentum configurations found in the propagators of the master topology

$$-\frac{1}{2} q \cdot (q - l) = \frac{1}{4} (-q^2 - (q - l)^2 + l^2), \quad (2.5)$$

or, in terms of the  $G$  integrals

$$I_1 = \frac{1}{4} \left( -G(0, 0, 0, 1, 1, 0, 1) - G(0, 1, 0, 0, 1, 0, 1) + G(0, 1, 0, 1, 1, -1, 1) \right), \quad (2.6)$$

where colour information has been stripped; this will be restored later. Another example is

$$I_5 = G(0, 1, 0, 1, 0, 0, 1) - G(0, 1, 0, 1, 0, 1, 0) - G(0, 1, 0, 1, 1, -1, 1) + G(0, 1, 0, 1, 1, 0, 0) - 2s G(0, 1, 0, 1, 1, 0, 1) \quad (2.7)$$

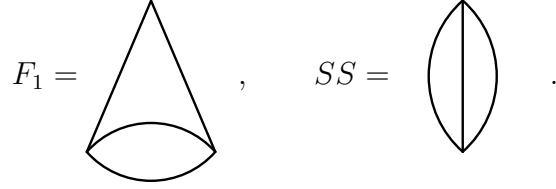
where  $s = (p_1 + p_2)^2$ .

We may then use the Laporta algorithm [22] and reduce these expressions to master integrals. We have used the software package FIRE [23] to achieve this. The results are

$$\begin{aligned} I_1 &= -\frac{s}{4} \frac{2\omega - 3}{3\omega - 4} F_1, & I_2 &= \frac{1}{4} \left( SS + \frac{3s}{2} \frac{2\omega - 3}{3\omega - 4} F_1 \right), \\ I_3 &= \frac{1}{2} (4\omega - 5) \left( \frac{1}{2\omega - 3} SS + \frac{s}{3\omega - 4} F_1 \right), \\ I_4 &= \frac{1}{2} I_3, & I_5 &= -\frac{s(4\omega - 5)}{3\omega - 4} F_1, \\ I_6 &= -\frac{1}{(4\pi)^{2\omega}} \frac{1}{s^{3-2\omega}} \left( \frac{\Gamma(2-\omega)\Gamma^2(\omega-1)}{\Gamma(2\omega-2)} \right)^2, \\ I_7 &= -4 I_1, \end{aligned} \quad (2.8)$$



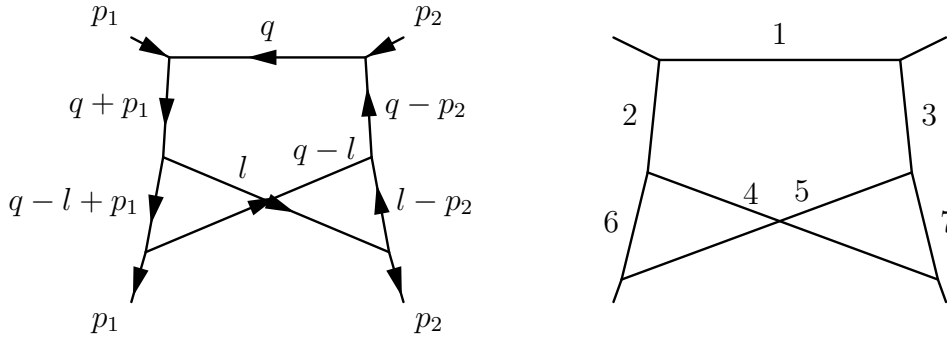
where the master integrals  $SS = G(0, 0, 1, 1, 1, 0, 0)$  and  $F_1 = G(0, 1, 0, 1, 1, 0, 1)$  may be visualized as follows



These integrals may be calculated in closed form by standard techniques

$$\begin{aligned}
 F_1 &= \frac{1}{(4\pi)^{2\omega}} \frac{1}{s^{4-2\omega}} \frac{\Gamma(4-2\omega)}{\Gamma(3\omega-4)} \Gamma(2-\omega) \Gamma^2(\omega-1) \frac{\Gamma(2\omega-3)}{2\omega-3}, \\
 SS &= \frac{1}{(4\pi)^{2\omega}} \frac{1}{s^{3-2\omega}} \frac{\Gamma(3-2\omega) \Gamma^3(\omega-1)}{\Gamma(3\omega-3)}.
 \end{aligned}
 \tag{2.9}$$

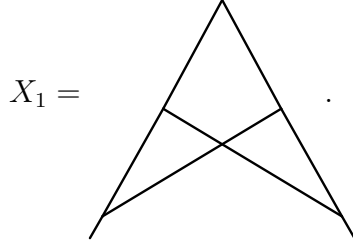
A crossed topology is required to reduce  $I_8$ , see appendix A.2. We use the following



and so associate an integral  $G(n_1, \dots, n_7)$  analogous to (2.4). We obtain

$$\begin{aligned}
 I_8 &= -\frac{s^3}{4} \frac{\omega-2}{4\omega-7} X_1 + \frac{1}{8} \left( 43 + \frac{12}{3-2\omega} + \frac{28}{(\omega-2)^2} + \frac{70}{\omega-2} + \frac{35}{4\omega-7} \right) SS \\
 &\quad + \frac{s}{24} \left( -37 + \frac{16}{4-3\omega} - \frac{30}{\omega-2} + \frac{15}{4\omega-7} \right) F_1,
 \end{aligned}
 \tag{2.10}$$

where  $X_1 = G(0, 1, 1, 1, 1, 1, 1)$  in this topology and may be visualized as follows



It is given by [24]

$$\begin{aligned}
X_1 = & \frac{1}{2s^{6-2\omega}} \frac{1}{(4\pi)^{2\omega}} \frac{\Gamma(5-2\omega)\Gamma(\omega-1)}{(\omega-2)^4} \left( \right. \\
& - \frac{\Gamma^2(\omega-1)}{\Gamma(3\omega-5)} {}_4F_3(1, \omega-1, 2\omega-4, 4\omega-8; 2\omega-3, 2\omega-3, 3\omega-5; 1) \\
& - 8 \frac{(\omega-2)^2 \Gamma(\omega-1) \Gamma(2\omega-3)}{(\omega-3)(2\omega-5) \Gamma(4\omega-7)} {}_3F_2(1, 1, 5-2\omega; 6-2\omega, 4-\omega; 1) \\
& + \frac{\Gamma(3-\omega) \Gamma(\omega-1) \Gamma(2\omega-3)}{\Gamma(3\omega-5)} {}_3F_2(1, 2\omega-4, 4\omega-8; 2\omega-3, 3\omega-5; 1) \\
& \left. - 2 \frac{\Gamma^2(5-2\omega) \Gamma(3-\omega) \Gamma^4(2\omega-3)}{\Gamma(9-4\omega) \Gamma^2(4\omega-7)} \right). \tag{2.11}
\end{aligned}$$

### 2.2.1 Colour factors

The colour structure of the ABJ(M) fields is as follows: Chern-Simons gauge fields are  $U(N)$  adjoints  $A_{ij}^\mu$  and  $U(M)$  adjoints  $\hat{A}_{\hat{i}\hat{j}}^\mu$  (with opposite-sign Chern-Simons level), where  $i, j = 1, \dots, N$  and  $\hat{i}, \hat{j} = 1, \dots, M$ . In the ABJM case  $N = M$ , while ABJ is defined by  $N \neq M$ . There are complex scalars with flavour group  $SU(4)$  ( $A$  is a fundamental  $SU(4)$  index) which transform in the bifundamental  $(N, \bar{N})$  of the two  $U(N)$  groups, i.e.  $(Y^A)_{i\hat{i}}$  and their anti-bifundamental  $(\bar{N}, N)$  conjugates  $(Y_A^\dagger)_{\hat{i}i}$ . There are accompanying complex two-component fermions  $(\psi_A)_{i\hat{i}}$  and  $(\psi^{\dagger A})_{\hat{i}i}$ . The action for the ABJ(M) theory is given in (A.1).

There are certain contributions to the  $J = 2$  case which are special, in that their analogues for the  $J > 2$  cases are non-planar. These are versions of  $I_1$ ,  $I_2$ ,  $I_6$ ,  $I_7$ , and<sup>4</sup>  $I_8$  where one of the exchanged particles must go “around the outside” of the graph, and therefore in the case that there are more than two external legs, would have to cross them and thus become non-planar. The fat graphs for these contributions are given in figure 1.

---

<sup>4</sup> $I_7$  and  $I_8$  have no normally planar version, and thus only contribute to the  $J = 2$  case.

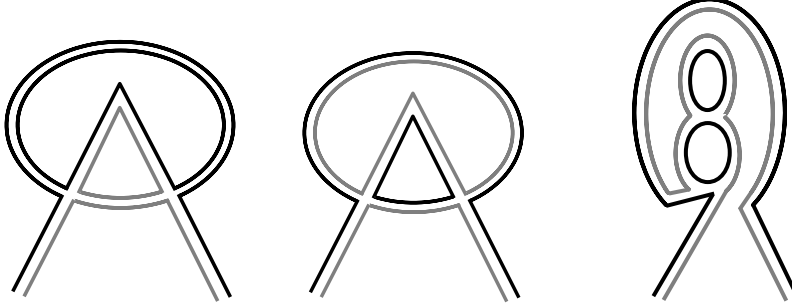


Figure 1: We show fat graphs for would-be-non-planar contributions to  $I_1$  (shown on the left),  $I_7$  (shown in the center), and  $I_6$  (shown on the right) where unhatted index lines are represented by a black line while hatted index lines are coloured gray. Note that  $I_2$  and  $I_8$  have topologies identical to  $I_1$ .

In the case of  $I_1$  and  $I_2$  the net effect of adding-in these would-be-non-planar contributions is a sign flip. The accounting for this is simple to see; the would-be-non-planar graphs involve one gluon of each flavour and therefore arise from cross-terms in the  $D_\mu Y^A D^\mu Y_A^\dagger$  part of the action. This means both a factor of two and a sign, relative to the contributions involving the same flavour of gluon, thus the net effect is  $1 - 2 = -1$ , or a flipped sign.

In the case of  $I_7$  there is a non-trivial flavour structure at play, however the rule  $I_7 = -4I_1$  continues to hold. The fermion-scalar vertices come in two varieties

$$\begin{aligned} V_1 &= \text{Tr} \left( Y^A Y_B^\dagger \psi_C \psi^{\dagger D} \right) \left( \delta_A^B \delta_D^C - 2\delta_D^B \delta_A^C \right), \\ V_2 &= -\text{Tr} \left( Y^A \psi^{\dagger B} Y^C \psi^{\dagger D} \right) \epsilon_{ABCD}, \end{aligned} \quad (2.12)$$

and (minus) their conjugates  $-\bar{V}_1$  and  $-\bar{V}_2$ . It is clear that we cannot take one of each variety in the graphs of interest to us, because the fields only propagate to their conjugates. For the diagram  $I_7$  the  $V_1$ - $\bar{V}_1$  contribution is proportional to the flavour trace, and so vanishes, whereas the would-be-non-planar contribution arises from the  $V_2$ - $\bar{V}_2$  combination. This involves a contraction of the two epsilon tensors on two indices, leaving both a flavour trace (which is zero) and an identity operator, which is not. The  $V_1$ - $V_1$  and  $\bar{V}_1$ - $\bar{V}_1$  contributions are truly non-planar, i.e. even in the  $J = 2$  case.

The case of  $I_6$  is different in that the would-be-non-planar contributions from  $V_1$ - $V_1$  and  $\bar{V}_1$ - $\bar{V}_1$  are in fact equal and opposite to the planar contributions from  $V_1$ - $\bar{V}_1$ . This cancellation eliminates the diagram  $I_6$  in the  $J = 2$  case.

The diagram  $I_8$  has no normally planar counter-part and thus only appears for  $J = 2$ .

### 2.2.2 Assembling the result

We now assemble the result of our calculation. Diagrams  $I_2$ ,  $I_3$ , and  $I_4$  receive a factor of two because we must add the left  $\leftrightarrow$  right versions of them. As explained above

the would-be-non-planar contributions flip the sign of  $I_1$  (and therefore implicitly  $I_7$  and  $I_2$ , and eliminate  $I_6$ . We therefore have that

$$F_{ABJM}(s) = 2 (4\pi\lambda)^2 \left( -I_1 - 2I_2 + 2I_3 + 2I_4 + I_5 + 0 \cdot I_6 - I_7 + I_8 \right), \quad (2.13)$$

where  $\lambda = N/k$  is the 't Hooft coupling and where the leading factor of two counts the two  $U(N)$  gauge groups, or equivalently the sum over the even and odd “sites” in the CPO.

Expanding (using the HypExp package [25]) in  $d = 2\omega = 3 - 2\epsilon$ , we find

$$F_{ABJM}(s) = \frac{\lambda^2}{2} \left( \frac{s e^\gamma}{4\pi} \right)^{-2\epsilon} \left( -\frac{1}{2\epsilon^2} - \frac{\log 2}{\epsilon} + 2 \log^2 2 + \frac{\pi^2}{3} + \mathcal{O}(\epsilon) \right). \quad (2.14)$$

It is also a straight-forward exercise to promote this result to the ABJ case, where the two gauge groups have different ranks. We define an extra 't Hooft coupling  $\hat{\lambda} = M/k$ , where  $M$  is the rank of one of the gauge groups, while the other remains  $N$ . By counting the light and dark gray index loops in diagrams like those shown in figure 1 we find

$$F_{ABJ}(s) = \left( \frac{4\pi}{k} \right)^2 \left( (M^2 + N^2 - 4MN)(I_1 + 2I_2) \right. \\ \left. + 2MN(I_3 + I_5 - I_7 + I_8) + (M^2 + N^2)(2I_4 + 0 \cdot I_6) \right), \quad (2.15)$$

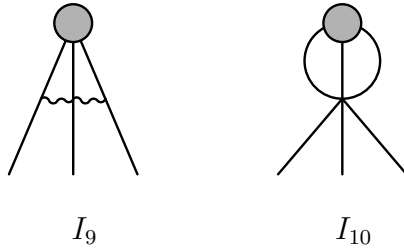
which upon expansion yields

$$F_{ABJ}(s) = \frac{1}{2} \left( \frac{s e^\gamma}{4\pi} \right)^{-2\epsilon} \left( -\frac{\lambda\hat{\lambda}}{2\epsilon^2} - (\lambda^2 + \hat{\lambda}^2) \frac{\log 2}{2\epsilon} + (\lambda^2 + \hat{\lambda}^2) \log^2 2 \right. \\ \left. + \left( \lambda^2 + \hat{\lambda}^2 + 6\lambda\hat{\lambda} \right) \frac{\pi^2}{24} + \mathcal{O}(\epsilon) \right). \quad (2.16)$$

We note that both the ABJM result in (2.14) and the ABJ result in (2.16) respect the principle of maximal transcendentality.

### 2.3 $J > 2$ case

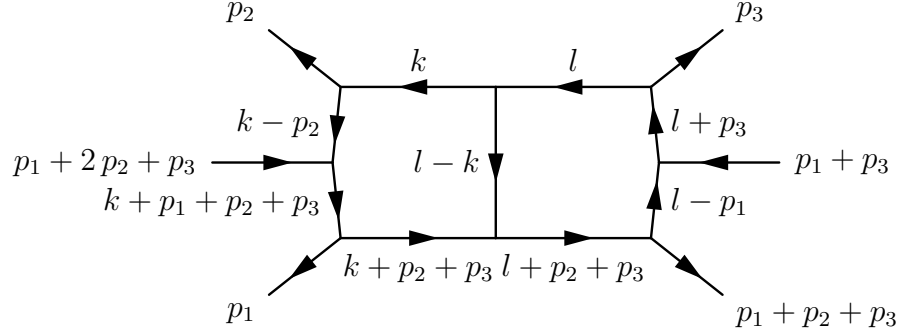
Here we will encounter two new diagrams, shown below for the case  $J = 3$  ( $J$  must be even, this is just for visualization purposes)<sup>5</sup>



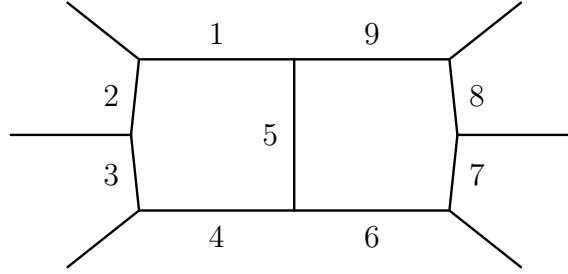

---

<sup>5</sup>The diagram corresponding to two separate gluon exchanges between legs 1 and 2, and legs 2 and 3 vanishes, see appendix A.3.

The master topology we need for these graphs is



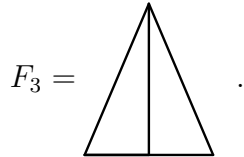
where we label propagators as



and associate a two-loop integral analogous to (2.4) which we call  $G(n_1, \dots, n_9)$ . Using the effective rule of eq. (A.7) of [21] (reproduced here in appendix A), and the FIRE package, we find the following result

$$I_9 = -\frac{1}{4} \frac{1}{(2\omega - 3)(3\omega - 5)} \left[ (50 + 2\omega(12\omega - 35)) \left( SS(s_{23}) - SS(s_{12} + s_{13} + s_{23}) + SS(s_{12}) \right) + (2\omega - 4)^2 s_{12} s_{23} F_3 \right], \quad (2.17)$$

where  $F_3 = G(0, 0, 1, 1, 1, 0, 0, 1, 1)$  and may be visualized by the following figure



This integral has been provided in eq. (5.27) of [26]. The result is

$$\begin{aligned}
F_3 &= \frac{(3\omega - 4)(3\omega - 5) SS(1)}{(\omega - 2)^2 s_{12}s_{23}} \\
&\times \left[ - \left( \frac{s_{12}s_{23}}{s_{13} + s_{23}} \right)^{2\omega-3} {}_2F_1 \left( 2\omega - 3, 2\omega - 3, 2\omega - 2, \frac{s_{13}}{s_{13} + s_{23}} \right) \right. \\
&\quad - \left( \frac{s_{12}s_{23}}{s_{13} + s_{12}} \right)^{2\omega-3} {}_2F_1 \left( 2\omega - 3, 2\omega - 3, 2\omega - 2, \frac{s_{13}}{s_{13} + s_{12}} \right) \\
&\quad \left. + \left( \frac{s_{123}s_{12}s_{23}}{(s_{13} + s_{23})(s_{13} + s_{12})} \right)^{2\omega-3} {}_2F_1 \left( 2\omega - 3, 2\omega - 3, 2\omega - 2, \frac{s_{13}s_{123}}{(s_{13} + s_{12})(s_{13} + s_{23})} \right) \right],
\end{aligned} \tag{2.18}$$

where  $s_{123} = s_{12} + s_{23} + s_{13}$ . The diagram  $I_{10}$  is trivial

$$I_{10} = SS(s_{12} + s_{13} + s_{23}). \tag{2.19}$$

### 2.3.1 Flavour structure for $I_{10}$

The flavour structure of the six-vertex gives (see eq. (B.2) of [21])

$$\mathbf{1} - \frac{1}{2}P \tag{2.20}$$

where  $P$  permutes two nearest odd or even sites. Since the CPO is symmetric, this gives rise to an extra factor of  $1/2$  dressing  $I_{10}$ , see below.

### 2.3.2 Assembling the result

We must note that now that we have more than two legs, the diagrams  $I_7$  and  $I_8$  do not contribute at the planar level,  $I_6$  is not canceled-out, and there are not sign-flips on  $I_1$  and  $I_2$ . Thus we have that

$$F_{ABJM}(\{s_{ij}\}) = (4\pi\lambda)^2 \sum_{\substack{\text{even and odd sites} \\ \equiv \text{legs}}} \left( I_1 + 2(I_2 + I_3 + I_4) + I_5 + I_6 + I_9 + \frac{1}{2}I_{10} \right). \tag{2.21}$$

Expanding in  $\epsilon$ , we find that

$$\begin{aligned}
F_{ABJM}(\{s_{ij}\}) &= \frac{J\lambda^2}{4} \left( \frac{e^\gamma}{4\pi} \right)^{-2\epsilon} \left( -\frac{1}{2\epsilon^2} + \frac{1}{\epsilon} \frac{1}{J} \sum_{i=1}^J \log \frac{s_{ii+1}}{2} \right. \\
&\quad \left. + 2 \log^2 2 - \frac{\pi^2}{3} - \frac{1}{J} \sum_{i=1}^J \log \frac{s_{ii+1}}{4} \log s_{ii+1} - \text{Trans}_2(\{s_{ij}\}) + \mathcal{O}(\epsilon) \right),
\end{aligned} \tag{2.22}$$

where

$$\begin{aligned}
\text{Trans}_2(\{s_{ij}\}) = & \frac{1}{J} \sum_{i=1}^J \left( \log s_{ii+1} \log s_{i+1i+2} \right. \\
& - \log(s_{ii+1} + s_{ii+2}) \log(s_{ii+2} + s_{i+1i+2}) \\
& + \log \frac{(s_{ii+1} + s_{ii+2})(s_{ii+2} + s_{i+1i+2})}{s_{ii+1}s_{i+1i+2}} \log(s_{ii+1} + s_{i+1i+2} + s_{ii+2}) \\
& + \text{Li}_2 \frac{s_{ii+2}}{s_{ii+1} + s_{ii+2}} + \text{Li}_2 \frac{s_{ii+2}}{s_{i+1i+2} + s_{ii+2}} \\
& \left. + \text{Li}_2 \frac{(s_{ii+1} + s_{i+1i+2} + s_{ii+2})s_{ii+2}}{(s_{ii+1} + s_{ii+2})(s_{ii+2} + s_{i+1i+2})} \right).
\end{aligned} \tag{2.23}$$

The ABJ case can be similarly worked out, we find

$$\begin{aligned}
F_{ABJ}(\{s_{ij}\}) = & \left( \frac{4\pi}{k} \right)^2 \left[ \sum_{\text{odd sites}} \left( M^2 I_1 + 2(M^2 I_2 + MNI_3 + M^2 I_4) + MNI_5 \right. \right. \\
& \left. \left. + M^2 I_6 + MNI_9 + \frac{MN}{2} I_{10} \right) \right. \\
& + \sum_{\text{even sites}} \left( N^2 I_1 + 2(N^2 I_2 + MNI_3 + N^2 I_4) + MNI_5 \right. \\
& \left. \left. + N^2 I_6 + MNI_9 + \frac{MN}{2} I_{10} \right) \right],
\end{aligned} \tag{2.24}$$

which expands to give

$$\begin{aligned}
F_{ABJ}(\{s_{ij}\}) = & \frac{J}{4} \left( \frac{e^\gamma}{4\pi} \right)^{-2\epsilon} \left( -\frac{\lambda \hat{\lambda}}{2\epsilon^2} - \frac{\lambda^2 + \hat{\lambda}^2}{2\epsilon} \log 2 + \frac{\lambda \hat{\lambda}}{\epsilon} \frac{1}{J} \sum_{i=1}^J \log s_{ii+1} \right. \\
& + (\lambda^2 + \hat{\lambda}^2) \log^2 2 - \left( 11(\lambda^2 + \hat{\lambda}^2) - 14\lambda \hat{\lambda} \right) \frac{\pi^2}{24} \\
& + (\lambda^2 + \hat{\lambda}^2) \frac{1}{J} \sum_{i=1}^J \log 2 \log s_{ii+1} - \lambda \hat{\lambda} \frac{1}{J} \sum_{i=1}^J \log^2 s_{ii+1} \\
& \left. - \lambda \hat{\lambda} \text{Trans}_2(\{s_{ij}\}) + \mathcal{O}(\epsilon) \right).
\end{aligned} \tag{2.25}$$

We note that, as in the  $J = 2$  case, both the ABJM result in (2.22) and the ABJ result in (2.25) respect the principle of maximal transcendentality.

### 3 Discussion

We have computed the leading quantum correction to the form factors for scalar chiral primary operators in ABJ(M) to an equal number of scalar final states at leading order

in the ‘t Hooft coupling. Our results, given in (2.14), (2.16), (2.22), and (2.25) are seen to obey the principle of maximal transcendentality, in that the terms of  $\mathcal{O}(\epsilon^{-n})$  are of transcendentality  $2 - n$ . This is consistent with calculations both of scattering amplitudes [27–31] and, recently, with light-like Wilson loop computations [32] (see [33–36] for previous work) in the same theory.

There are several further directions which would be interesting pursue. Firstly, it would be nice to calculate the form factors for more general final states, i.e. final states involving general numbers of fermions and scalars. Such expressions should be able to be compactly expressed in terms of “super form factors”. At tree-level this should be accomplished by the application of the BCFW recursion relations [37] and use of the superamplitudes [37, 38] already developed/computed for ABJM.

The duality between colour and kinematics in scattering amplitudes [39] has also been discovered to extend to form factors of  $\mathcal{N} = 4$  SYM [40]. Recently a proposal for such a duality has been made for the scattering amplitudes of ABJM [41]. Thus, it would be very interesting to attempt to extend this to the form factors considered here.

There is also the question of equality between the form factors and open periodic light-like Wilson loops, developed for the case of  $\mathcal{N} = 4$  SYM in [14, 42]. Here there are subtleties owing to the lack of gauge invariance of the open Wilson loop, and a gauge-invariant statement is still lacking<sup>6</sup>. However, it is still worth pursuing this calculation, which has recently been sharpened in the closed-loop case in [32].

Finally, as emphasized in the introduction, the form factors presented here should be useful for calculating the correlation functions of the chiral primary operators, following the program of generalized unitarity as recently proposed in [11]. The calculation of the three-point functions at leading order is under active investigation by the author.

## Acknowledgements

The author thanks Johannes Henn, Gregory Korchemsky, Charlotte Kristjansen, Tristan McLoughlin, Jan Plefka, and Gordon Semenoff for discussions, and also thanks A. Brandhuber, Ö. Gürdoğan, D. Korres, R. Mooney and G. Travaglini for discussions and for sharing their manuscript prior to publication. The author also thanks J. A. Minahan, O. Ohlsson Sax, and C. Sieg for permission to use a figure from their paper. The author was supported in part by FNU through grant number 272-08-0329.

## A Computational details

We follow very closely the conventions of [21], however we evaluate the form factor in Euclidean signature. The regularization scheme is dimensional regularization with all products involving the three-dimensional Levi-Civita tensor reduced to scalar products prior to integration, which is known to be a healthy scheme [43].

---

<sup>6</sup>I thank G. Travaglini for a discussion on this point.



The action used in [21] is in Lorentzian mostly-positive signature, with the Levi-Civita tensor defined as  $\epsilon^{012} = 1$  and  $\gamma^\mu\gamma^\nu = \eta_{\mu\nu} + \epsilon_{\mu\nu\rho}\gamma^\rho$

$$\begin{aligned}
S = \frac{k}{4\pi} \text{Tr} \int d^3x \left[ \epsilon^{\mu\nu\rho} \left( A_\mu \partial_\nu A_\rho + \frac{2i}{3} A_\mu A_\nu A_\rho \right) - \epsilon^{\mu\nu\rho} \left( \hat{A}_\mu \partial_\nu \hat{A}_\rho + \frac{2i}{3} \hat{A}_\mu \hat{A}_\nu \hat{A}_\rho \right) \right. \\
- D_\mu Y_A^\dagger D^\mu Y^A + i\psi^\dagger \gamma^\mu D_\mu \psi_A \\
+ \frac{1}{12} Y^A Y_B^\dagger Y^C Y_D^\dagger Y^E Y_F^\dagger (\delta_A^B \delta_C^D \delta_E^F + \delta_A^F \delta_C^B \delta_E^D - 6\delta_A^B \delta_C^F \delta_E^D + 4\delta_A^D \delta_C^F \delta_E^B) \\
- \frac{i}{2} (Y_A^\dagger Y^B \psi^\dagger \psi_D - \psi_D \psi^\dagger Y^B Y_A^\dagger) (\delta_B^A \delta_C^D - 2\delta_C^A \delta_B^D) \\
\left. + \frac{i}{2} \epsilon^{ABCD} Y_A^\dagger \psi_B Y_C^\dagger \psi_D - \frac{i}{2} \epsilon_{ABCD} Y^A \psi^\dagger B Y^C \psi^\dagger D \right], \tag{A.1}
\end{aligned}$$

where  $D_\mu Y^A = \partial_\mu Y^A + iA_\mu Y^A - iY^A \hat{A}_\mu$  and  $D_\mu Y_A^\dagger = \partial_\mu Y_A^\dagger - iY_A^\dagger A_\mu + i\hat{A}_\mu Y_A^\dagger$  and similarly for the fermions. Further details about the action are available in [21].

The effective Feynman rules are reproduced below, with permission from [21].

The Feynman diagrams and their corresponding mathematical expressions are as follows:

- $\text{Diagram 1} = \frac{1}{2} \text{Diagram 2}$
- $\text{Diagram 3} = \frac{1}{2} \left( \text{Diagram 4} - \text{Diagram 5} \right) = 0$
- $\text{Diagram 6} = - \text{Diagram 7} + \text{Diagram 8}$
- $\text{Diagram 9} = - \text{Diagram 10} + \text{Diagram 11} = 0$
- $\text{Diagram 12} = 2 \left( - \text{Diagram 13} + \text{Diagram 14} \right) = 0$
- $\text{Diagram 15} = 4 \left( \text{Diagram 16} - \text{Diagram 17} - \text{Diagram 18} + \text{Diagram 19} + \text{Diagram 20} - \text{Diagram 21} \right)$
- $\text{Diagram 22} = 2 \left( - \text{Diagram 23} + \text{Diagram 24} + \text{Diagram 25} + \text{Diagram 26} - \text{Diagram 27} \right)$
- $\text{Diagram 28} = 4 \left( \text{Diagram 29} - \text{Diagram 30} \right)$
- $\text{Diagram 31} = -2 \text{Diagram 32}$

$$\begin{aligned}
\left| \begin{array}{c} \text{---} \\ \text{---} \\ \text{---} \end{array} \right| &= 2i \left( - \begin{array}{c} \uparrow \\ \text{---} \\ \downarrow \end{array} + \begin{array}{c} \uparrow \\ \text{---} \\ \downarrow \end{array} \right), \\
\left| \begin{array}{c} \text{---} \\ \text{---} \\ \text{---} \end{array} \right| &= 4i \left( \begin{array}{c} \uparrow \\ \text{---} \\ \downarrow \end{array} - \begin{array}{c} \uparrow \\ \text{---} \\ \downarrow \end{array} + \begin{array}{c} \uparrow \\ \text{---} \\ \downarrow \end{array} - \begin{array}{c} \uparrow \\ \text{---} \\ \downarrow \end{array} + \begin{array}{c} \uparrow \\ \text{---} \\ \downarrow \end{array} - \begin{array}{c} \uparrow \\ \text{---} \\ \downarrow \end{array} \right).
\end{aligned}$$

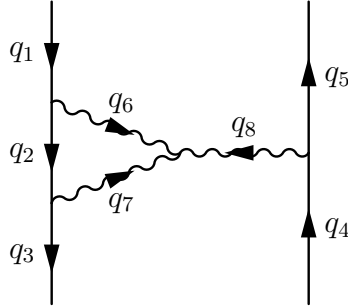
Gluons are represented by wiggly lines, scalars by plain lines, and fermions by dashed lines. The filled blob corresponds to the 1-loop correction to the gluon propagator. On the right hand side are the effective rules, where arrows appear in pairs and indicate contracted momenta of the two associated lines. When two gluons appear on opposite sides of a scalar line, they belong to opposite gauge groups.

The procedure for translating these rules to Euclidean signature is to multiply by  $-i$  for every propagator on the left hand side and to divide by  $-i$  for every vertex on the left hand side. This just removes the  $i$ 's from the last two rules above and leaves all other rules unaffected.

The overall coupling assumed in these rules is  $4\pi/k$ , and hence the two-loop calculation of the form factors presented here require multiplication by  $(4\pi/k)^2$  times the relevant colour factors.

### A.1 Effective rule for $I_4$

We find that the effective rule given in [21] for  $I_4$  gives inconsistent results in our case. This is likely because of  $0/0$  limits when the bottom two legs are taken on-shell (the calculation in [21] is for an off-shell quantity)<sup>7</sup>. For this reason we prefer to use the direct evaluation given below



$$= -\frac{1}{4}(q_1 + q_2)^\mu (q_2 + q_3)^\nu (q_4 + q_5)^\lambda q_6^\phi q_7^\xi q_8^\omega \epsilon^{\alpha\beta\gamma} \epsilon_{\mu\phi\alpha} \epsilon_{\nu\xi\beta} \epsilon_{\lambda\omega\gamma},$$

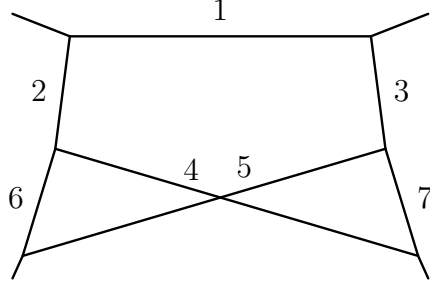
where the result is understood to be multiplied by the propagators of the off-shell lines and integrated over the loop momenta. The contractions of the epsilon tensors must be replaced by scalar products prior to integration.

### A.2 Effective rule for $I_8$

An effective Feynman rule for the crossed-topology diagram  $I_8$  is not provided in [21]. Rather than attempt to derive one ourselves we decided to simply use the direct

<sup>7</sup>I thank C. Sieg for discussions on this point.

evaluation of the numerators. The result is as follows, where the  $q_i$  momenta refer to the labels in the master topology, which is reproduced from the main text below

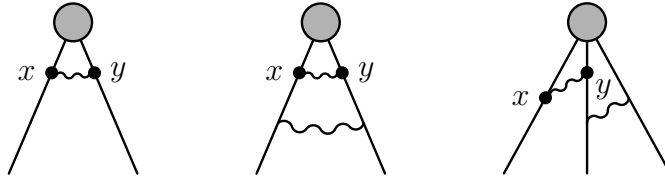


$$I_8 = -\frac{1}{4} \left[ (q_2 + q_6) \wedge q_4 \wedge (q_7 - p_2) \right] \left[ (p_1 + q_6) \wedge q_5 \wedge (q_7 + q_3) \right] G(0, 1, 1, 1, 1, 1, 1, 1),$$

where the triple wedge-product indicates contraction with the Levi-Civita tensor. The product of two such triple products must be re-expressed as scalar products of momenta prior to evaluation using the usual identity.

### A.3 On the vanishing of certain diagrams

There is a simple way to see that the following diagrams are zero on the physical dimension (and so are at most  $\mathcal{O}(\epsilon)$  in dimensional regularization; we have verified that they are, in fact, exactly zero)



where we can also imagine an arbitrary number of additional legs emanating from the operator – the legs shown are assumed to be adjacent. We consider the one-gluon exchange across two legs of the operator, and we work in position space. To illustrate we have marked the two ends of the gluon exchange with their space-time coordinates in the diagrams above. We take the operator to lie at the origin. The gluon exchange will contribute the following expression

$$\text{gluon exchange} \propto \partial_x P(x) \wedge \partial_x P(x - y) \wedge \partial_y P(y) \quad (\text{A.2})$$

where the triple-wedge product indicates contraction with the Levi-Civita tensor, and  $P(z) \sim 1/z$  is the position-space scalar propagator. The partial derivatives come from the scalar couplings to the gluon and from the gluon propagator. This expression vanishes since it is proportional to  $x \wedge (x - y) \wedge y$ .

## References

- [1] N. Beisert, C. Ahn, L. F. Alday, Z. Bajnok, J. M. Drummond, *et al.*, “Review of AdS/CFT Integrability: An Overview,” *Lett.Math.Phys.* **99** (2012) 3–32, [arXiv:1012.3982 \[hep-th\]](#).
- [2] Z. Bern, L. J. Dixon, and V. A. Smirnov, “Iteration of planar amplitudes in maximally supersymmetric Yang-Mills theory at three loops and beyond,” *Phys.Rev.* **D72** (2005) 085001, [arXiv:hep-th/0505205 \[hep-th\]](#).
- [3] L. F. Alday and J. M. Maldacena, “Gluon scattering amplitudes at strong coupling,” *JHEP* **0706** (2007) 064, [arXiv:0705.0303 \[hep-th\]](#).
- [4] J. Drummond, J. Henn, G. Korchemsky, and E. Sokatchev, “Dual superconformal symmetry of scattering amplitudes in N=4 super-Yang-Mills theory,” *Nucl.Phys.* **B828** (2010) 317–374, [arXiv:0807.1095 \[hep-th\]](#).
- [5] J. M. Drummond, J. M. Henn, and J. Plefka, “Yangian symmetry of scattering amplitudes in N=4 super Yang-Mills theory,” *JHEP* **0905** (2009) 046, [arXiv:0902.2987 \[hep-th\]](#).
- [6] O. Aharony, O. Bergman, D. L. Jafferis, and J. Maldacena, “N=6 superconformal Chern-Simons-matter theories, M2-branes and their gravity duals,” *JHEP* **0810** (2008) 091, [arXiv:0806.1218 \[hep-th\]](#).
- [7] P. Caputa and B. A. E. Mohammed, “From Schurs to Giants in ABJ(M),” *JHEP* **1301** (2013) 055, [arXiv:1210.7705 \[hep-th\]](#).
- [8] S. Hirano, C. Kristjansen, and D. Young, “Giant Gravitons on  $AdS_4 \times CP^3$  and their Holographic Three-point Functions,” *JHEP* **1207** (2012) 006, [arXiv:1205.1959 \[hep-th\]](#).
- [9] D. Correa, J. Maldacena, and A. Sever, “The quark anti-quark potential and the cusp anomalous dimension from a TBA equation,” *JHEP* **1208** (2012) 134, [arXiv:1203.1913 \[hep-th\]](#).
- [10] V. Cardinali, L. Griguolo, G. Martelloni, and D. Seminara, “New supersymmetric Wilson loops in ABJ(M) theories,” [arXiv:1209.4032 \[hep-th\]](#).
- [11] O. T. Engelund and R. Roiban, “Correlation functions of local composite operators from generalized unitarity,” [arXiv:1209.0227 \[hep-th\]](#).
- [12] W. van Neerven, “INFRARED BEHAVIOR OF ON-SHELL FORM-FACTORS IN A N=4 SUPERSYMMETRIC YANG-MILLS FIELD THEORY,” *Z.Phys.* **C30** (1986) 595.
- [13] K. Selivanov, “On tree form-factors in (supersymmetric) Yang-Mills theory,” *Commun.Math.Phys.* **208** (2000) 671–687, [arXiv:hep-th/9809046 \[hep-th\]](#).

- [14] A. Brandhuber, B. Spence, G. Travaglini, and G. Yang, “Form Factors in N=4 Super Yang-Mills and Periodic Wilson Loops,” *JHEP* **1101** (2011) 134, [arXiv:1011.1899 \[hep-th\]](#).
- [15] A. Brandhuber, O. Gurdogan, R. Mooney, G. Travaglini, and G. Yang, “Harmony of Super Form Factors,” *JHEP* **1110** (2011) 046, [arXiv:1107.5067 \[hep-th\]](#).
- [16] A. Brandhuber, G. Travaglini, and G. Yang, “Analytic two-loop form factors in N=4 SYM,” *JHEP* **1205** (2012) 082, [arXiv:1201.4170 \[hep-th\]](#).
- [17] L. Bork, D. Kazakov, and G. Vartanov, “On form factors in N=4 sym,” *JHEP* **1102** (2011) 063, [arXiv:1011.2440 \[hep-th\]](#).
- [18] L. Bork, D. Kazakov, and G. Vartanov, “On MHV Form Factors in Superspace for  $\mathcal{N} = 4$  SYM Theory,” *JHEP* **1110** (2011) 133, [arXiv:1107.5551 \[hep-th\]](#).
- [19] O. Aharony, O. Bergman, and D. L. Jafferis, “Fractional M2-branes,” *JHEP* **0811** (2008) 043, [arXiv:0807.4924 \[hep-th\]](#).
- [20] A. Brandhuber, O. Gurdogan, D. Korres, R. Mooney, and G. Travaglini, “Two-loop Sudakov Form Factor in ABJM,” [arXiv:1305.2421 \[hep-th\]](#).
- [21] J. Minahan, O. Ohlsson Sax, and C. Sieg, “Anomalous dimensions at four loops in N=6 superconformal Chern-Simons theories,” *Nucl.Phys.* **B846** (2011) 542–606, [arXiv:0912.3460 \[hep-th\]](#).
- [22] S. Laporta, “High precision calculation of multiloop Feynman integrals by difference equations,” *Int.J.Mod.Phys.* **A15** (2000) 5087–5159, [arXiv:hep-ph/0102033 \[hep-ph\]](#).
- [23] A. Smirnov, “Algorithm FIRE – Feynman Integral REduction,” *JHEP* **0810** (2008) 107, [arXiv:0807.3243 \[hep-ph\]](#).
- [24] T. Gehrmann, T. Huber, and D. Maitre, “Two-loop quark and gluon form-factors in dimensional regularisation,” *Phys.Lett.* **B622** (2005) 295–302, [arXiv:hep-ph/0507061 \[hep-ph\]](#).
- [25] T. Huber and D. Maitre, “HypExp: A Mathematica package for expanding hypergeometric functions around integer-valued parameters,” *Comput.Phys.Commun.* **175** (2006) 122–144, [arXiv:hep-ph/0507094 \[hep-ph\]](#).
- [26] T. Gehrmann and E. Remiddi, “Differential equations for two loop four point functions,” *Nucl.Phys.* **B580** (2000) 485–518, [arXiv:hep-ph/9912329 \[hep-ph\]](#).
- [27] A. Agarwal, N. Beisert, and T. McLoughlin, “Scattering in Mass-Deformed  $N \geq 4$  Chern-Simons Models,” *JHEP* **0906** (2009) 045, [arXiv:0812.3367 \[hep-th\]](#).

- [28] W.-M. Chen and Y.-t. Huang, “Dualities for Loop Amplitudes of N=6 Chern-Simons Matter Theory,” *JHEP* **1111** (2011) 057, [arXiv:1107.2710 \[hep-th\]](#).
- [29] T. Bargheer, N. Beisert, F. Loebbert, T. McLoughlin, N. Beisert, *et al.*, “Conformal Anomaly for Amplitudes in N=6 Superconformal Chern-Simons Theory,” *J.Phys.* **A45** (2012) 475402, [arXiv:1204.4406 \[hep-th\]](#).
- [30] M. S. Bianchi, M. Leoni, A. Mauri, S. Penati, and A. Santambrogio, “One Loop Amplitudes In ABJM,” *JHEP* **1207** (2012) 029, [arXiv:1204.4407 \[hep-th\]](#).
- [31] S. Caron-Huot and Y.-t. Huang, “The two-loop six-point amplitude in ABJM theory,” *JHEP* **1303** (2013) 075, [arXiv:1210.4226 \[hep-th\]](#).
- [32] M. S. Bianchi, G. Giribet, M. Leoni, and S. Penati, “Light-like Wilson loops in ABJM and maximal transcendentality,” [arXiv:1304.6085 \[hep-th\]](#).
- [33] J. M. Henn, J. Plefka, and K. Wiegandt, “Light-like polygonal Wilson loops in 3d Chern-Simons and ABJM theory,” *JHEP* **1008** (2010) 032, [arXiv:1004.0226 \[hep-th\]](#).
- [34] M. S. Bianchi, M. Leoni, A. Mauri, S. Penati, C. Ratti, *et al.*, “From Correlators to Wilson Loops in Chern-Simons Matter Theories,” *JHEP* **1106** (2011) 118, [arXiv:1103.3675 \[hep-th\]](#).
- [35] M. S. Bianchi, M. Leoni, A. Mauri, S. Penati, and A. Santambrogio, “Scattering Amplitudes/Wilson Loop Duality In ABJM Theory,” *JHEP* **1201** (2012) 056, [arXiv:1107.3139 \[hep-th\]](#).
- [36] K. Wiegandt, “Equivalence of Wilson Loops in  $\mathcal{N} = 6$  super Chern-Simons matter theory and  $\mathcal{N} = 4$  SYM Theory,” *Phys.Rev.* **D84** (2011) 126015, [arXiv:1110.1373 \[hep-th\]](#).
- [37] D. Gang, Y.-t. Huang, E. Koh, S. Lee, and A. E. Lipstein, “Tree-level Recursion Relation and Dual Superconformal Symmetry of the ABJM Theory,” *JHEP* **1103** (2011) 116, [arXiv:1012.5032 \[hep-th\]](#).
- [38] T. Bargheer, F. Loebbert, and C. Meneghelli, “Symmetries of Tree-level Scattering Amplitudes in N=6 Superconformal Chern-Simons Theory,” *Phys.Rev.* **D82** (2010) 045016, [arXiv:1003.6120 \[hep-th\]](#).
- [39] Z. Bern, J. Carrasco, and H. Johansson, “New Relations for Gauge-Theory Amplitudes,” *Phys.Rev.* **D78** (2008) 085011, [arXiv:0805.3993 \[hep-ph\]](#).
- [40] R. H. Boels, B. A. Kniehl, O. V. Tarasov, and G. Yang, “Color-kinematic Duality for Form Factors,” *JHEP* **1302** (2013) 063, [arXiv:1211.7028 \[hep-th\]](#).

- [41] T. Bargheer, S. He, and T. McLoughlin, “New Relations for Three-Dimensional Supersymmetric Scattering Amplitudes,” *Phys.Rev.Lett.* **108** (2012) 231601, arXiv:1203.0562 [hep-th].
- [42] L. F. Alday and J. Maldacena, “Comments on gluon scattering amplitudes via AdS/CFT,” *JHEP* **0711** (2007) 068, arXiv:0710.1060 [hep-th].
- [43] W. Chen, G. W. Semenoff, and Y.-S. Wu, “Two loop analysis of nonAbelian Chern-Simons theory,” *Phys.Rev.* **D46** (1992) 5521–5539, arXiv:hep-th/9209005 [hep-th].